

Coulomb instabilities of 3D higher-order topological insulators

Peng-Lu Zhao,¹ Xiao-Bin Qiang,¹ Hai-Zhou Lu,^{1,2,*} and X. C. Xie^{3,4,5}

¹Shenzhen Institute for Quantum Science and Engineering and Department of Physics, Southern University of Science and Technology (SUSTech), Shenzhen 518055, China

²Shenzhen Key Laboratory of Quantum Science and Engineering, Shenzhen 518055, China

³International Center for Quantum Materials, School of Physics, Peking University, Beijing 100871, China

⁴CAS Center for Excellence in Topological Quantum Computation, University of Chinese Academy of Sciences, Beijing 100190, China

⁵Beijing Academy of Quantum Information Sciences, West Building 3, No. 10, Xibeiwang East Road, Haidian District, Beijing 100193, China

(Dated: March 4, 2021)

Topological insulator is an exciting discovery because of its robustness against disorder and interactions. Recently, higher-order topological insulators have been attracting increasing attention, because they host 1D topologically-protected hinge states in 3D or 0D corner states in 2D. A significantly critical issue is whether the higher-order topological insulators also survive interactions, but it is still unexplored. We study the effects of weak Coulomb interaction on 3D second-order topological insulators, with the help of a renormalization group calculation. We find that the higher-order topological insulators are always unstable, suffering from two types of topological phase transitions. One is from higher-order topological insulator to first-order topological insulator, the other is to normal insulator. The first type is accompanied by emergent time-reversal and inversion symmetries and has a dynamical critical exponent $z = 1$. The second type does not have the emergent symmetries and has non-universal dynamical critical exponents $z < 1$. Our results may inspire more inspections on the stability of higher-order topological states of matter and related novel quantum criticalities.

Introduction.—As a generalization of the topological insulator [1–12], higher-order topological insulators have been attracting considerable interest recently [13–25]. A simplest 3D higher-order topological insulator hosts 3D gapped bulk states inside but topologically protected gapless 1D hinge states and gapped 2D surface states (Fig. 1). There have been experimental evidences for the higher-order topology in bosonic systems, including circuitry [26–28], phononics [29], acoustics [30–32], and photonics [33–36]. Despite the theoretical predictions on material candidates [18, 19, 37–40], there are few direct observation of higher-order topological insulators in electronic systems [19]. This raises the concerns on the stability of higher-order topological insulators against, *e.g.* disorder [41–43]. More importantly, it is still unknown whether higher-order topological insulators can survive a more intrinsic presence in electronic systems, the Coulomb interaction [44–55].

In this Letter, we study the stability of 3D higher-order topological insulators in the present of the Coulomb interaction. We find that the higher-order topological insulators are always unstable. Two types of topological phase transition could happen (Fig. 1). In the first type, the Coulomb interaction could drive a topological phase transition from higher-order topological insulator to first-order topological insulator. This transition is accompanied by the recovery of time-reversal and inversion symmetries in the low-energy limit, and hence is protected by these emergent symmetries. The quantum criticality for this phase transition is described by a dynamical critical exponent $z = 1$ and a correlation length exponent

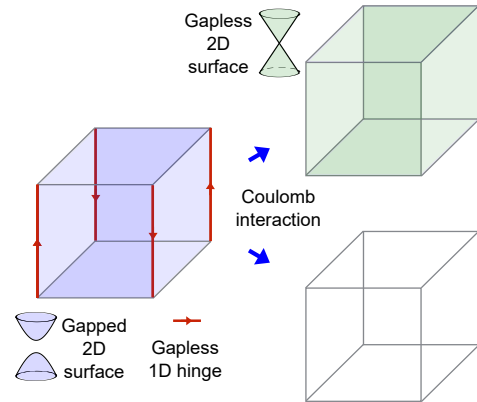


FIG. 1. Schematic of a typical 3D second-order topological insulator (left) which hosts 3D gapped bulk states in the interior but topologically protected 2D massive (gapped) Dirac cones on the surfaces and gapless 1D chiral hinge states. It may turn to a topological insulator (right top) or a normal insulator (right bottom), in the presence of the Coulomb interaction.

$\nu = 1$. In the second type, the Coulomb interaction could induce another topological phase transition from higher-order topological insulator to normal insulator. There are no emergent symmetry when this phase transition happens, and its criticality is characterized by the appearance of non-universal dynamical critical exponents $z < 1$. Our results will be insightful for the ongoing experimental search for higher-order topological insulators in electronic systems.

Model for 3D second-order topological insulator.—We

start with a four-band Hamiltonian for 3D second-order topological insulators [18],

$$\mathcal{H}_0(\mathbf{k}) = [M + t \sum_i \cos(ak_i)] \tau_z \sigma_0 + \Delta_1 \sum_i \sin(ak_i) \tau_x \sigma_i + \Delta_2 [\cos(ak_x) - \cos(ak_y)] \tau_y \sigma_0, \quad (1)$$

where $i = x, y, z$, a is the lattice constant and σ_i and τ_i are the Pauli matrices. M, t, Δ_1, Δ_2 are the hopping parameters. This model has no time-reversal symmetry if $\Delta_2 \neq 0$ (Sec. SI of [56]). Also, a four-fold rotation symmetry on the $x-y$ plane by the operator $R_{4z} \equiv \tau_0 e^{-i\frac{\pi}{4}\sigma_z}$ is broken by the nonzero Δ_2 term. The combination $R_{4z}\mathcal{T}$ (\mathcal{T} is the time-reversal operator) is a symmetry of Hamiltonian, and this symmetry protects the existence of the 3D second-order topological insulator. Another important symmetry is the combination of time reversal and inversion \mathcal{IT} (Sec. SII of [56]), where $\mathcal{I} = \tau_z \sigma_0$. With the \mathcal{IT} symmetry, one can identify the \mathcal{Z}_2 invariants by

$$(-1)^\nu = \prod_i \prod_{n=1}^{N/2} \xi_n(\Gamma_i), \quad (2)$$

where $\xi_n(\Gamma_i) = \pm 1$ is the eigenvalue of \mathcal{I} for the n th occupied energy band at momenta Γ_i , and $\Gamma_i \in \{(0, 0, 0), (\pi, \pi, 0), (0, 0, \pi), (\pi, \pi, \pi)\}$ representing all the $R_{4z}\mathcal{T}$ -invariant \mathbf{k} points. As a result, for $1 < |M/t| < 3$, $(-1)^\nu = -1$ (Sec. SII of [56]), which represents the second-order topological insulator phase and for $|M/t| > 3$ or $|M/t| < 1$, $(-1)^\nu = 1$, which stands for the topologically-trivial band insulator phase (normal insulator). This difference establishes only when $\Delta_1 \neq 0 \neq \Delta_2$. Once $\Delta_1 = 0$, there exist gapless points which break the insulating nature. Once $\Delta_2 = 0$, time-reversal symmetry recovers and Hamiltonian Eq. (1) describes the well-known 3D topological insulator if $1 < |M/t| < 3$. Later, we will show that in the presence of Coulomb interaction, even if we take $\Delta_2 \neq 0$ and $1 < |M/t| < 3$ at the beginning, Δ_2 will flow to zero in the low-energy limit, leading to a topological phase transition from higher-order topological insulator to topological insulator. Moreover, the Coulomb interaction could also drive $|M/t|$ to exceed 3, which induces a transition from topological insulator to normal insulator.

Coulomb interaction and renormalization group equations.—The low-energy effective action in Euclidean spacetime for a 3D second-order topological insulator in the presence of the Coulomb interaction takes the form

$$\mathcal{S} = \int d\tau d^3\mathbf{r} \{ \bar{\psi} [(\partial_\tau + ig\phi) \gamma_0 + v\boldsymbol{\gamma} \cdot \boldsymbol{\partial} + m + B\partial^2 - iD(\partial_x^2 - \partial_y^2) \gamma_5] \psi + \frac{1}{2} \sum_{i=x,y,z} \eta_i (\partial_i \phi)^2 \}, \quad (3)$$

where ψ describes a four-component fermion field and $\bar{\psi} = \psi^\dagger \gamma_0$. The γ matrices satisfy the anticommuting algebra $\{\gamma_\mu, \gamma_\nu\} = 2\delta_{\mu,\nu}$. $v = \Delta_1 a, m = M + 3t, B = ta^2/2$,

and $D = \Delta_2 a^2/2$, which are obtained by expanding Eq. (1) around the Γ point. The parameter v represents the Fermi velocity, m is the Dirac mass, and terms involving B and D represent the quadratic corrections to the Dirac Hamiltonian. We have introduced an auxiliary scale field ϕ through the Hubbard-Stratonovich transformation [57] to decouple the density-density Coulomb interaction, $(\eta_x, \eta_y, \eta_z) = (1, 1, \eta)$ is used to characterize the spatial anisotropy of ϕ , and $g = e/\sqrt{\epsilon}$ representing the coupling between electrons and the scalar field, where $-e$ is the electron charge, and ϵ is the dielectric constant. The Coulomb interaction does not break the $R_{4z}\mathcal{T}$ and \mathcal{IT} symmetries of Eq. (1) (Sec. SIIIA of [56]), and the topology is still distinguished by Eq. (2). According to Eq. (1), the gap closing and reopening is controlled solely by m [3, 9, 58], and the topological phase transition between higher-order topological insulator and normal insulator is identified by a sign change of m .

To explore how the Coulomb interaction renormalizes the band parameters and consequently changes the stability of the topological phases, we perform a Wilsonian momentum-shell renormalization group analysis [59] for the model described by Eq. (3). The momentum shell is defined by $e^{-\ell}\Lambda < |\mathbf{k}| < \Lambda$, where ℓ is the running scale parameter. With increasing ℓ , the energy scale is lowered, and the lowest energy limit corresponds to $\ell \rightarrow +\infty$. After redefining the original band parameters B, D, m, v and Coulomb interaction strength g into dimensionless

$$B\Lambda v^{-1} \rightarrow B, D\Lambda v^{-1} \rightarrow D, mv^{-1}\Lambda^{-1} \rightarrow m, g^2/4\pi^2 v \rightarrow \alpha, \quad (4)$$

the renormalization group flow equations for these dimensionless parameters are found as (Sec. SIIIC of [56])

$$\frac{dv}{d\ell} = (z - 1 + \alpha\mathcal{F}_1) v, \quad (5)$$

$$\frac{dm}{d\ell} = m + \alpha [(m - B)\mathcal{F}_0 - m\mathcal{F}_1], \quad (6)$$

$$\frac{dB}{d\ell} = -B + \alpha [(B - m)\mathcal{F}_2 - B\mathcal{F}_1], \quad (7)$$

$$\frac{dD}{d\ell} = [\alpha(\mathcal{F}_3 - \mathcal{F}_1) - 1] D, \quad (8)$$

$$\frac{d\alpha}{d\ell} = -\alpha^2 (2\mathcal{F}_0 - 2\mathcal{F}_1 + \mathcal{F}_4), \quad (9)$$

$$\frac{d\eta}{d\ell} = \alpha (\mathcal{F}_5 - \eta\mathcal{F}_4 + 6\eta\mathcal{F}_1 - 4\eta\mathcal{F}_0), \quad (10)$$

where $\mathcal{F}_{i=0-6}$ are dimensionless functions of m, B, D , and η , whose explicit expressions are presented in Sec. IIIB of [56]. z is the dynamic exponent whose value is obtained by fixing v . We numerically solve the above coupled renormalization group equations and obtain the running of m, B, D, α, η and z with ℓ . Despite that the running of these parameters are highly dependent on their initial values, *i.e.* their values at the cutoff Λ , we find their behaviors can be classified into two categories, corresponding to two types of phase transitions.

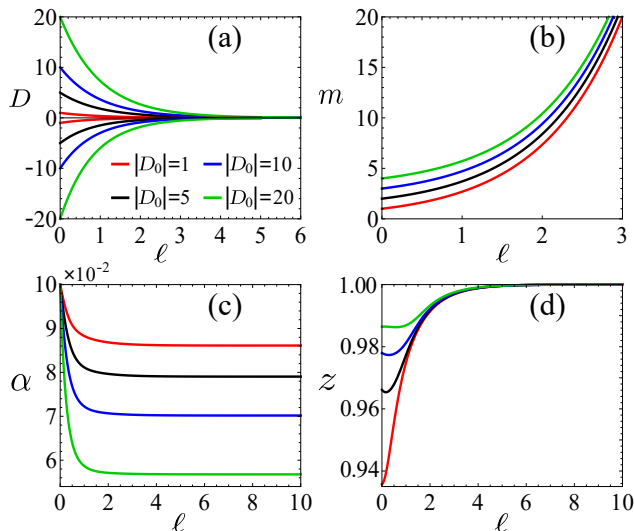


FIG. 2. (a)–(c) Numerical solutions to the renormalized D , m , and α as functions of the running scale parameter ℓ . D and m protect the second-order and first-order topological properties, respectively. The vanishing D and increasing m means a topological phase transition from 3D second-order to topological insulator. (d) The scale dependence of z . The solutions are obtained by fixing the values at $\ell = 0$ ($|\mathbf{p}| = \Lambda$) as $m_0 = B_0 = 1$, $\alpha_0 = 0.1$, $\eta_0 = 0.8$ but varying D_0 . (a)–(d) share the same legends. In (b), the $m(\ell)$ curve of $D_0 = 5, 10$, and 20 are shifted vertically by 1 for clarity.

From second-order to first-order topological insulator.–

This topological phase transition is characterized by a vanishing D and always positive m at large ℓ (the low-energy limit). We show the existence of this case in Fig. 2. Figure 2(a) shows that, in a large range of D_0 , D flows to zero rapidly with increasing ℓ . This behavior reflects that the renormalization group equation for D [Eq. (8)] only has one stable fixed point at $D_* = 0$. As D flows to zero, m increases and remains positive, which is shown in Fig. 2(b). The unrestricted growth of m ceases the rapid decay of α [see Fig. 2(c)] because $\mathcal{F}_{0,1} \sim 1/|m|$, $\mathcal{F}_4 \sim 1/|m|^3$ for extremely large m , which give rises to $d\alpha/d\ell \sim 0$. Although the effective Coulomb interaction is marginally irrelevant according to Eq. (9), its values in the low-energy limit is a small constant instead of zero [see Fig. 2(c)]. Without changing the sign of m , there is no gap closing and reopening near the Γ point when approaching the low-energy limit, and the topological invariant does not change. However, when D flows to zero, the free part of the effective model Eq. (3) reduces to the modified Dirac Hamiltonian that describes 3D topological insulators [7, 9]. According to the previous results [45, 60–62], 3D topological insulators are immune to weak Coulomb interaction. Therefore, the low-energy state is a topological insulator with finite but weak Coulomb interaction, which means that the second-order topological insulator is unstable in the presence of Coulomb interaction. Concomitant with the topological phase transition

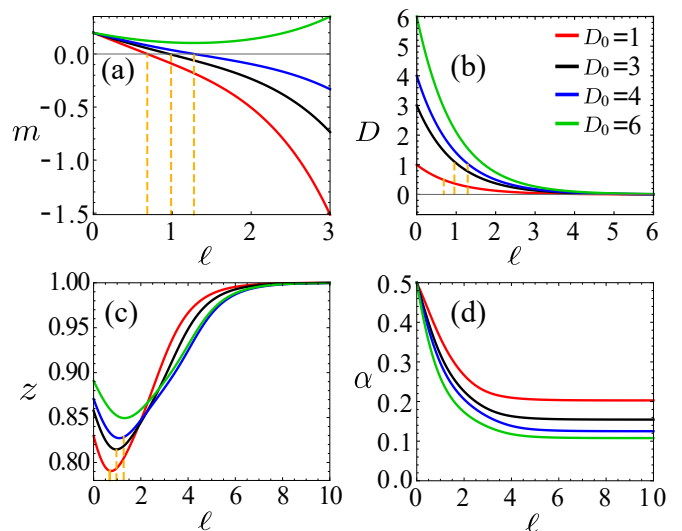


FIG. 3. (a), (b), (d) Numerical solutions to the renormalized m , D , and α as functions of the running scale parameter ℓ . D and m protect the second-order and first-order topological properties, respectively. The finite D at the sign change of m means a topological phase transition from 3D second-order topological insulator to normal insulator. (c) The scale dependence of z . The solutions are obtained by varying the initial value D and fixing the initial values of other parameters as $m_0 = 0.2$, $B_0 = 2$, $\alpha_0 = 0.5$, and $\eta_0 = 0.8$. (a)–(d) share the same legends. The orange dashed lines in (a)–(c) label the values of ℓ at which the topological phase transitions happen. In (b) and (c), the crossing points of the orange dashed lines with the red, black, blue lines indicate the values of D and z when the topological phase transitions happen. From left to right, the corresponding values are 0.49, 1.09, 1.05 for D in (b) and 0.79, 0.81, 0.83 for z in (c).

from second-order to topological insulator, time-reversal symmetry and inversion symmetry emerge. The previous works has shown the possibility of emergent Lorentz symmetry [63–70], emergent chiral symmetry [71–73], and even emergent supersymmetry [74–85]. Here, by providing the concrete example, we show that emergent symmetries could happen for the discrete time-reversal and inversion symmetries, which enrich the family of emergent symmetries [86]. The occurrence of this topological phase transition does not need a large critical value of α . In Sec. IV of [56], we show that this phase transition exists at least for $\alpha \sim 10^{-3}$, which corresponds to extremely weak Coulomb interaction. We find that the dynamical critical exponent $z = 1$ for this phase transition, as shown in Fig. 2(d). We also obtain a correlation length exponent $\nu = 1$ by assuming that the spatial correlation length ξ diverges as $\delta \equiv D - D_* \rightarrow 0$ in the manner $\xi \sim |\delta|^{-\nu}$. This definition is similar to the conventional definition of the correlation length exponent in a symmetry broken quantum phase transition [87, 88].

From second-order topological insulator to normal insulator.–This topological phase transition is character-

ized by a sign change of m and a constant D as m changes sign. Here, a constant D means that it cannot be viewed as zero approximately, which guarantees the topological phase transition to normal insulator happens before the transition to topological insulator. We show the existence of this kind of behaviors for m and D in Fig. 3. Figure 3(a) shows that m will change sign when D_0 is below a critical value. For comparison, the green line shows a case in which m does not change sign. Figure 3(b) shows that the value of D does not vanish when m changes sign. Therefore, for the parameters represented by the red, black and blue lines in Fig. 3(a), the topological phase transition from second-order topological insulators to normal insulators happens and for the case depicted by the green line the topological phase transition from second-order to first-order topological insulator happens, which has been discussed previously. Due to the finite D at the phase transition point, there is no emergent symmetry. After the phase transition, the emergent time-reversal and inversion symmetries appear in the low-energy limit of the normal insulator. An interesting property of this topological phase transition is the non-universal value of the dynamical critical exponent. As shown in Fig. 3(c), the values of the dynamical critical exponents are different for the three cases, all below 1. A non-universal $z < 1$ is a direct result of the phase transition happening at a finite energy scale ℓ . According to Eq. (5),

$$z(\ell) = 1 - \alpha(\ell) \mathcal{F}_1(\ell). \quad (11)$$

The values of $\alpha(\ell)$ are always positive constant [see Fig. 3(d)], and the non-negative $\mathcal{F}_1(\ell)$ vanishes only at $\ell \rightarrow \infty$. Considering that the sign change of m always happens at a finite ℓ , the value of z will be less than 1 and its particular value depends on the values of α and $\mathcal{F}_1(\ell)$, and hence is non-universal. However, as shown in Fig. 3(c), the asymptotic value of z for $\ell \rightarrow \infty$ is still 1, which describes the low-energy dynamics of the normal insulator.

Phase diagrams.—We have shown our main results by varying the initial values of D and fixing the other band parameters as constants. We could do similar analyses for any cases by changing one parameter while fixing others in our renormalization-group equations, but our conclusions do not change. To give a global view of the dependences of the phases and phase transitions on the band parameters and interaction strength, we plot the phase diagrams as functions of α , D , B , and m in Fig. 4. Based on Fig. 4(b) and (d), we find that the value of m plays a key role to determine the type of phase transition. Once m is large enough [for example $m_c \approx 0.535$ in Fig. 4(d)], only the phase transition to topological insulator exists and the transition to normal insulator is suppressed. Due to the dominant role of m , our conclusions also apply to other 3D higher-order topological insulators, for example, the helical second-order topo-

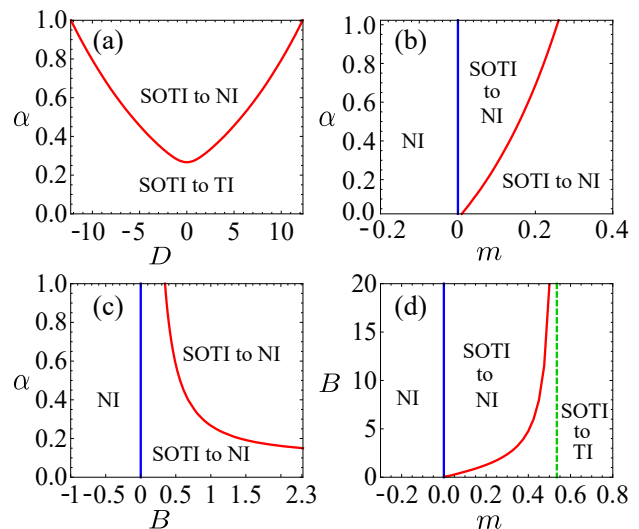


FIG. 4. Phase diagrams in the D - α plane (a), m - α plane (b), B - α plane (c) and m - B plane (d). TI, BI, and SOTI stand for (first-order) topological insulator, normal insulator, and second-order topological insulator, respectively. The blue and red lines are the boundaries of the phases. The dashed green line in (d) labels $m_c \approx 0.535$. When $m > m_c$, only the SOTI to TI phase transition could happen. The other parameters are fixed at $B_0 = 10m_0 = 1$ in (a), $B_0 = D_0 = 1$ in (b), $D_0 = m_0 = 0.1$ in (c), $D_0 = \alpha_0 = 0.5$ in (d), and $\eta_0 = 0.8$ in all the diagrams.

logical insulator [18]. In particular, the 3D higher-order topological insulators require breaking of time-reversal symmetry and keeping a combined n -fold rotational and time-reversal symmetry $R_{ni}\mathcal{T}$ ($n = 2, 4, 6; i = x, y, z$) to quantize the electric multipoles [13, 14, 18]. In a band theory Hamiltonian, the terms with the $R_{ni}\mathcal{T}$ symmetry must appear as anisotropic quadratic or higher-order corrections to the Dirac Hamiltonian (for example, the term with D in our model). According to our calculation, these terms are all irrelevant in the low-energy limit, and as a result, the transition to topological insulator happens. The transition from high-order topological insulator to normal insulator originates from the interplay between the isotropic quadratic term (B) and the Dirac mass term (m) generated by the Coulomb interaction, which does not depend on the terms protecting the high-order topological insulators and hence will still exist for other 3D higher-order topological insulators.

Discussion.—Our results show that the Coulomb interaction is critical in the experiments searching for higher-order topological insulators. Previously, the transition between topological and normal insulators has been observed in $\text{BiTl}(\text{S}_{1-\delta}\text{Se}_\delta)_2$ [89] by varying δ . Our theory shares a similar spirit, by fixing the values of the band parameters at the cutoff and analyzing their behaviors at a particular low energy scale. As a result, the change of initial values of the band parameters is equivalent to the change of the parameters at the particular

energy scale relevant to the experiment. Therefore, the topological phase transitions from higher-order to normal and topological insulators are possible to be observed in experiments by doping the recently-proposed candidate materials of high-order topological insulators, including bismuth [19], EuIn_2As_2 [39], and MnBi_2Te_4 [40]. Correspondingly, the 1D gapless hinge state will transform into a gapped state or two-dimensional Dirac cone, which could be observed in experiments.

We thank helpful discussions with Jing-Rong Wang and Daoyuan Li. This work was supported by the National Natural Science Foundation of China (12047531, 11534001, 11974249, 11925402), the Strategic Priority Research Program of Chinese Academy of Sciences (XDB28000000), Guangdong province (2016ZT06D348, 2017ZT07C062, and 2020KCXTD001), the National Key R & D Program (2016YFA0301700), Shenzhen High-level Special Fund (G02206304, G02206404), and the Science, Technology and Innovation Commission of Shenzhen Municipality (ZDSYS20190902092905285, ZDSYS20170303165926217, JCYJ20170412152620376, KYTDPT20181011104202253). The numerical calculations were supported by Center for Computational Science and Engineering of Southern University of Science and Technology.

* Corresponding author: luhz@sustech.edu.cn

- [1] L. Fu, C. L. Kane, and E. J. Mele, Topological Insulators in Three Dimensions, *Phys. Rev. Lett.* **98**, 106803 (2007).
- [2] J. E. Moore and L. Balents, Topological invariants of time-reversal-invariant band structures, *Phys. Rev. B* **75**, 121306 (2007).
- [3] S. Murakami, Phase transition between the quantum spin Hall and insulator phases in 3D: emergence of a topological gapless phase, *New J. Phys.* **9**, 356 (2007).
- [4] R. Roy, Topological phases and the quantum spin Hall effect in three dimensions, *Phys. Rev. B* **79**, 195322 (2009).
- [5] L. Fu and C. L. Kane, Topological insulators with inversion symmetry, *Phys. Rev. B* **76**, 045302 (2007).
- [6] D. Hsieh, D. Qian, L. Wray, Y. Xia, Y. S. Hor, R. J. Cava, and M. Z. Hasan, A topological Dirac insulator in a quantum spin Hall phase, *Nature* **452**, 970 (2008).
- [7] H. Zhang, C.-X. Liu, X.-L. Qi, X. Dai, Z. Fang, and S.-C. Zhang, Topological insulators in Bi_2Se_3 , Bi_2Te_3 and Sb_2Te_3 with a single Dirac cone on the surface, *Nat. Phys.* **5**, 438 (2009).
- [8] Y. Xia, D. Qian, D. Hsieh, L. Wray, A. Pal, H. Lin, A. Bansil, D. Grauer, Y. S. Hor, R. J. Cava, and M. Z. Hasan, Observation of a large-gap topological-insulator class with a single Dirac cone on the surface, *Nat. Phys.* **5**, 398 (2009).
- [9] S.-Q. Shen, *Topological Insulators*, 2nd ed. (Springer-Verlag, Berlin Heidelberg, 2017).
- [10] M. Z. Hasan and C. L. Kane, Colloquium: Topological insulators, *Rev. Mod. Phys.* **82**, 3045 (2010).
- [11] X.-L. Qi and S.-C. Zhang, Topological insulators and superconductors, *Rev. Mod. Phys.* **83**, 1057 (2011).
- [12] M. Z. Hasan and J. E. Moore, Three-Dimensional Topological Insulators, *Annu. Rev. Condens. Matter Phys.* **2**, 55 (2011).
- [13] W. A. Benalcazar, B. A. Bernevig, and T. L. Hughes, Quantized electric multipole insulators, *Science* **357**, 61 (2017).
- [14] W. A. Benalcazar, B. A. Bernevig, and T. L. Hughes, Electric multipole moments, topological multipole moment pumping, and chiral hinge states in crystalline insulators, *Phys. Rev. B* **96**, 245115 (2017).
- [15] Z. Song, Z. Fang, and C. Fang, $(d - 2)$ -Dimensional Edge States of Rotation Symmetry Protected Topological States, *Phys. Rev. Lett.* **119**, 246402 (2017).
- [16] C. M. Wang, H.-P. Sun, H.-Z. Lu, and X. C. Xie, 3D Quantum Hall Effect of Fermi Arcs in Topological Semimetals, *Phys. Rev. Lett.* **119**, 136806 (2017).
- [17] J. Langbehn, Y. Peng, L. Trifunovic, F. von Oppen, and P. W. Brouwer, Reflection-Symmetric Second-Order Topological Insulators and Superconductors, *Phys. Rev. Lett.* **119**, 246401 (2017).
- [18] F. Schindler, A. M. Cook, M. G. Vergniory, Z. Wang, S. S. P. Parkin, B. A. Bernevig, and T. Neupert, Higher-order topological insulators, *Sci. Adv.* **4**, 6 (2018).
- [19] F. Schindler, Z. Wang, M. G. Vergniory, A. M. Cook, A. Murani, S. Sengupta, A. Y. Kasumov, R. Deblock, S. Jeon, I. Drozdov, H. Bouchiat, S. Guéron, A. Yazdani, B. A. Bernevig, and T. Neupert, Higher-order topology in bismuth, *Nat. Phys.* **14**, 918 (2018).
- [20] M. Ezawa, Higher-Order Topological Insulators and Semimetals on the Breathing Kagome and Pyrochlore Lattices, *Phys. Rev. Lett.* **120**, 026801 (2018).
- [21] Z. Li, Y. Cao, P. Yan, and X. Wang, Higher-order topological solitonic insulators, *npj Comput. Mater.* **5**, 107 (2019).
- [22] T. Liu, Y.-R. Zhang, Q. Ai, Z. Gong, K. Kawabata, M. Ueda, and F. Nori, Second-Order Topological Phases in Non-Hermitian Systems, *Phys. Rev. Lett.* **122**, 076801 (2019).
- [23] X.-W. Luo and C. Zhang, Higher-Order Topological Corner States Induced by Gain and Loss, *Phys. Rev. Lett.* **123**, 073601 (2019).
- [24] K. Kudo, T. Yoshida, and Y. Hatsugai, Higher-Order Topological Mott Insulators, *Phys. Rev. Lett.* **123**, 196402 (2019).
- [25] R. Chen, C.-Z. Chen, J.-H. Gao, B. Zhou, and D.-H. Xu, Higher-Order Topological Insulators in Quasicrystals, *Phys. Rev. Lett.* **124**, 036803 (2020).
- [26] C. W. Peterson, W. A. Benalcazar, T. L. Hughes, and G. Bahl, A quantized microwave quadrupole insulator with topologically protected corner states, *Nature* **555**, 346 (2018).
- [27] S. Imhof, C. Berger, F. Bayer, J. Brehm, L. W. Molenkamp, T. Kiessling, F. Schindler, C. H. Lee, M. Greiter, T. Neupert, and R. Thomale, Topoelectrical-circuit realization of topological corner modes, *Nat. Phys.* **14**, 925 (2018).
- [28] M. Serra-Garcia, R. Süssstrunk, and S. D. Huber, Observation of quadrupole transitions and edge mode topology in an LC circuit network, *Phys. Rev. B* **99**, 020304(R) (2019).
- [29] M. Serra-Garcia, V. Peri, R. Süssstrunk, O. R. Bilal, T. Larsen, L. G. Villanueva, and S. D. Huber, Observation of a phononic quadrupole topological insulator, *Nature* **555**, 342 (2018).

- [30] H. Xue, Y. Yang, F. Gao, Y. Chong, and B. Zhang, Acoustic higher-order topological insulator on a kagome lattice, *Nat. Mater.* **18**, 108 (2019).
- [31] X. Ni, M. Weiner, A. Alù, and A. B. Khanikaev, Observation of higher-order topological acoustic states protected by generalized chiral symmetry, *Nat. Mater.* **18**, 113 (2019).
- [32] H. Xue, Y. Ge, H. X. Sun, Q. Wang, D. Jia, Y. J. Guan, S. Q. Yuan, Y. Chong, and B. Zhang, Observation of an acoustic octupole topological insulator, *Nat. Commun.* **11**, 2442 (2020).
- [33] S. Mittal, V. V. Orre, G. Zhu, M. A. Gorlach, A. Poddubny, and M. Hafezi, Photonic quadrupole topological phases, *Nat. Photonics* **13**, 692 (2019).
- [34] A. El Hassan, F. K. Kunst, A. Moritz, G. Andler, E. J. Bergholtz, and M. Bourennane, Corner states of light in photonic waveguides, *Nat. Photonics* **13**, 697 (2019).
- [35] B.-Y. Xie, G.-X. Su, H.-F. Wang, H. Su, X.-P. Shen, P. Zhan, M.-H. Lu, Z.-L. Wang, and Y.-F. Chen, Visualization of higher-order topological insulating phases in two-dimensional dielectric photonic crystals, *Phys. Rev. Lett.* **122**, 233903 (2019).
- [36] M. Li, D. Zhirihin, M. Gorlach, X. Ni, D. Filonov, A. Slobozhanyuk, A. Alù, and A. B. Khanikaev, Higher-order topological states in photonic kagome crystals with long-range interactions, *Nat. Photonics* **14**, 89 (2020).
- [37] C. Yue, Y. Xu, Z. Song, H. Weng, Y. M. Lu, C. Fang, and X. Dai, Symmetry-enforced chiral hinge states and surface quantum anomalous Hall effect in the magnetic axion insulator $\text{Bi}_{2-x}\text{Sm}_x\text{Se}_3$, *Nat. Phys.* **15**, 577 (2019).
- [38] Z. Wang, B. J. Wieder, J. Li, B. Yan, and B. A. Bernevig, Higher-Order Topology, Monopole Nodal Lines, and the Origin of Large Fermi Arcs in Transition Metal Dichalcogenides XTe_2 ($\text{X}=\text{Mo}, \text{W}$), *Phys. Rev. Lett.* **123**, 186401 (2019).
- [39] Y. Xu, Z. Song, Z. Wang, H. Weng, and X. Dai, Higher-Order Topology of the Axion Insulator EuIn_2As_2 , *Phys. Rev. Lett.* **122**, 256402 (2019).
- [40] R. X. Zhang, F. Wu, and S. Das Sarma, Möbius Insulator and Higher-Order Topology in $\text{MnBi}_{2n}\text{Te}_{3n+1}$, *Phys. Rev. Lett.* **124**, 136407 (2020).
- [41] Z. Su, Y. Kang, B. Zhang, Z. Zhang, and H. Jiang, Disorder induced phase transition in magnetic higher-order topological insulator: A machine learning study, *Chin. Phys. B* **28**, 117301 (2019).
- [42] C. Wang and X. R. Wang, Disorder-Induced Quantum Phase Transitions in Three-Dimensional Second-Order Topological Insulators, *Phys. Rev. Research* **2**, 033521 (2020).
- [43] C. A. Li, B. Fu, Z. A. Hu, J. Li, and S. Q. Shen, Topological Phase Transitions in Disordered Electric Quadrupole Insulators, *Phys. Rev. Lett.* **125**, 166801 (2020).
- [44] J. González, F. Guinea, and M. A. H. Vozmediano, Marginal-Fermi-liquid behavior from two-dimensional Coulomb interaction, *Phys. Rev. B* **59**, R2474 (1999).
- [45] P. Goswami and S. Chakravarty, Quantum Criticality between Topological and Band Insulators in $3+1$ Dimensions, *Phys. Rev. Lett.* **107**, 196803 (2011).
- [46] P. Hosur, S. A. Parameswaran, and A. Vishwanath, Charge Transport in Weyl Semimetals, *Phys. Rev. Lett.* **108**, 046602 (2012).
- [47] E.-G. Moon, C. Xu, Y. B. Kim, and L. Balents, Non-Fermi-Liquid and Topological States with Strong Spin-Orbit Coupling, *Phys. Rev. Lett.* **111**, 206401 (2013).
- [48] B.-J. Yang, E.-G. Moon, H. Isobe, and N. Nagaosa, Quantum criticality of topological phase transitions in three-dimensional interacting electronic systems, *Nat. Phys.* **10**, 774 (2014).
- [49] J. Hofmann, E. Barnes, and S. Das Sarma, Why Does Graphene Behave as a Weakly Interacting System?, *Phys. Rev. Lett.* **113**, 105502 (2014).
- [50] H.-H. Lai, Correlation effects in double-Weyl semimetals, *Phys. Rev. B* **91**, 235131 (2015).
- [51] S.-K. Jian and H. Yao, Correlated double-Weyl semimetals with Coulomb interactions: Possible applications to HgCr_2Se_4 and SrSi_2 , *Phys. Rev. B* **92**, 045121 (2015).
- [52] Y. Huh, E.-G. Moon, and Y. B. Kim, Long-range Coulomb interaction in nodal-ring semimetals, *Phys. Rev. B* **93**, 035138 (2016).
- [53] H. Isobe, B.-J. Yang, A. Chubukov, J. Schmalian, and N. Nagaosa, Emergent Non-Fermi-Liquid at the Quantum Critical Point of a Topological Phase Transition in Two Dimensions, *Phys. Rev. Lett.* **116**, 076803 (2016).
- [54] G. Y. Cho and E.-G. Moon, Novel Quantum Criticality in Two Dimensional Topological Phase transitions, *Sci. Rep.* **6**, 19198 (2016).
- [55] H. Isobe and N. Nagaosa, Coulomb Interaction Effect in Weyl Fermions with Tilted Energy Dispersion in Two Dimensions, *Phys. Rev. Lett.* **116**, 116803 (2016).
- [56] See Supplemental Material for details.
- [57] P. Coleman, *Introduction to Many-Body Physics* (Cambridge University Press, Cambridge, 2015).
- [58] S.-Q. Shen, W.-Y. Shan, and H.-Z. Lu, Topological insulator and the Dirac equation, *SPIN* **01**, 33 (2011).
- [59] R. Shankar, Renormalization-group approach to interacting fermions, *Rev. Mod. Phys.* **66**, 129 (1994).
- [60] X.-L. Qi, T. L. Hughes, and S.-C. Zhang, Topological field theory of time-reversal invariant insulators, *Phys. Rev. B* **78**, 195424 (2008).
- [61] Z. Wang, X. L. Qi, and S. C. Zhang, Topological order parameters for interacting topological insulators, *Phys. Rev. Lett.* **105**, 256803 (2010).
- [62] Z. Wang, X. L. Qi, and S. C. Zhang, Topological invariants for interacting topological insulators with inversion symmetry, *Phys. Rev. B* **85**, 165126 (2012).
- [63] H. Nielsen and M. Ninomiya, β -Function in a non-covariant Yang-Mills theory, *Nucl. Phys. B* **141**, 153 (1978).
- [64] S. Chadha and H. Nielsen, Lorentz invariance as a low energy phenomenon, *Nucl. Phys. B* **217**, 125 (1983).
- [65] M. Sitte, A. Rosch, J. S. Meyer, K. A. Matveev, and M. Garst, Emergent lorentz symmetry with vanishing velocity in a critical two-subband quantum wire, *Phys. Rev. Lett.* **102**, 176404 (2009).
- [66] M. M. Anber and J. F. Donoghue, Emergence of a universal limiting speed, *Phys. Rev. D* **83**, 105027 (2011).
- [67] G. Bednik, O. Pujolàs, and S. Sibiryakov, Emergent lorentz invariance from strong dynamics: holographic examples, *J. High Energy Phys.* **2013**, 64 (2013).
- [68] S. Sibiryakov, From scale invariance to lorentz symmetry, *Phys. Rev. Lett.* **112**, 241602 (2014).
- [69] I. V. Kharuk and S. M. Sibiryakov, Emergent lorentz invariance with chiral fermions, *Theor. Math. Phys.* **189**, 1755 (2016).
- [70] B. Roy, V. Juricić, and I. F. Herbut, Emergent Lorentz symmetry near fermionic quantum critical points in two and three dimensions, *J. High Energy Phys.* **2016**, 18 (2016).

- [71] A. P. Balachandran and S. Vaidya, Emergent Chiral Symmetry: Parity and Time Reversal Doubles, *Int. J. Mod. Phys. A* **12**, 5325 (1997).
- [72] D. R. Candido, M. Kharitonov, J. C. Egues, and E. M. Hankiewicz, Paradoxical extension of the edge states across the topological phase transition due to emergent approximate chiral symmetry in a quantum anomalous hall system, *Phys. Rev. B* **98**, 161111 (2018).
- [73] A. L. Szabó and B. Roy, Emergent chiral symmetry in a three-dimensional interacting Dirac liquid, *J. High Energy Phys.* **2021**, 4 (2021).
- [74] L. Balents, M. P. A. Fisher, and C. Nayak, Nodal Liquid Theory of the Pseudo-Gap Phase of High-Tc Superconductors, *Int. J. Mod. Phys. B* **12**, 1033 (1998).
- [75] P. Fendley, K. Schoutens, and J. de Boer, Lattice Models with $\mathcal{N} = 2$ Supersymmetry, *Phys. Rev. Lett.* **90**, 120402 (2003).
- [76] S.-S. Lee, Emergence of supersymmetry at a critical point of a lattice model, *Phys. Rev. B* **76**, 075103 (2007).
- [77] Y. Yu and K. Yang, Supersymmetry and the Goldstino-Like Mode in Bose-Fermi Mixtures, *Phys. Rev. Lett.* **100**, 090404 (2008).
- [78] Y. Yu and K. Yang, Simulating the Wess-Zumino Supersymmetry Model in Optical Lattices, *Phys. Rev. Lett.* **105**, 150605 (2010).
- [79] B. Bauer, L. Huijse, E. Berg, M. Troyer, and K. Schoutens, Supersymmetric multicritical point in a model of lattice fermions, *Phys. Rev. B* **87**, 165145 (2013).
- [80] T. Grover, D. N. Sheng, and A. Vishwanath, Emergent Space-Time Supersymmetry at the Boundary of a Topological Phase, *Science* **344**, 280 (2014).
- [81] P. Ponte and S.-S. Lee, Emergence of supersymmetry on the surface of three-dimensional topological insulators, *New J. Phys.* **16**, 013044 (2014).
- [82] S.-K. Jian, Y.-F. Jiang, and H. Yao, Emergent space-time supersymmetry in 3d weyl semimetals and 2d dirac semimetals, *Phys. Rev. Lett.* **114**, 237001 (2015).
- [83] S.-K. Jian, C.-H. Lin, J. Maciejko, and H. Yao, Emergence of supersymmetric quantum electrodynamics, *Phys. Rev. Lett.* **118**, 166802 (2017).
- [84] P. Feldmann, A. Wipf, and L. Zambelli, Critical wess-zumino models with four supercharges in the functional renormalization group approach, *Phys. Rev. D* **98**, 096005 (2018).
- [85] P.-L. Zhao and G.-Z. Liu, Absence of emergent supersymmetry at superconducting quantum critical points in dirac and weyl semimetals, *npj Quantum Mater.* **4**, 37 (2019).
- [86] G. Volovik, Emergent physics: Fermi-point scenario, *Phil. Trans. R. Soc. A* **366**, 2935 (2008).
- [87] S. L. Sondhi, S. M. Girvin, J. P. Carini, and D. Shahar, Continuous quantum phase transitions, *Rev. Mod. Phys.* **69**, 315 (1997).
- [88] M. Imada, A. Fujimori, and Y. Tokura, Metal-insulator transitions, *Rev. Mod. Phys.* **70**, 1039 (1998).
- [89] S.-Y. Xu, Y. Xia, L. A. Wray, S. Jia, F. Meier, J. H. Dil, J. Osterwalder, B. Slomski, A. Bansil, H. Lin, R. J. Cava, and M. Z. Hasan, Topological phase transition and texture inversion in a tunable topological insulator, *Science* **332**, 560 (2011).